GNSS as a tool for tropospheric water vapor monitoring. Alqueva lake Case-Study

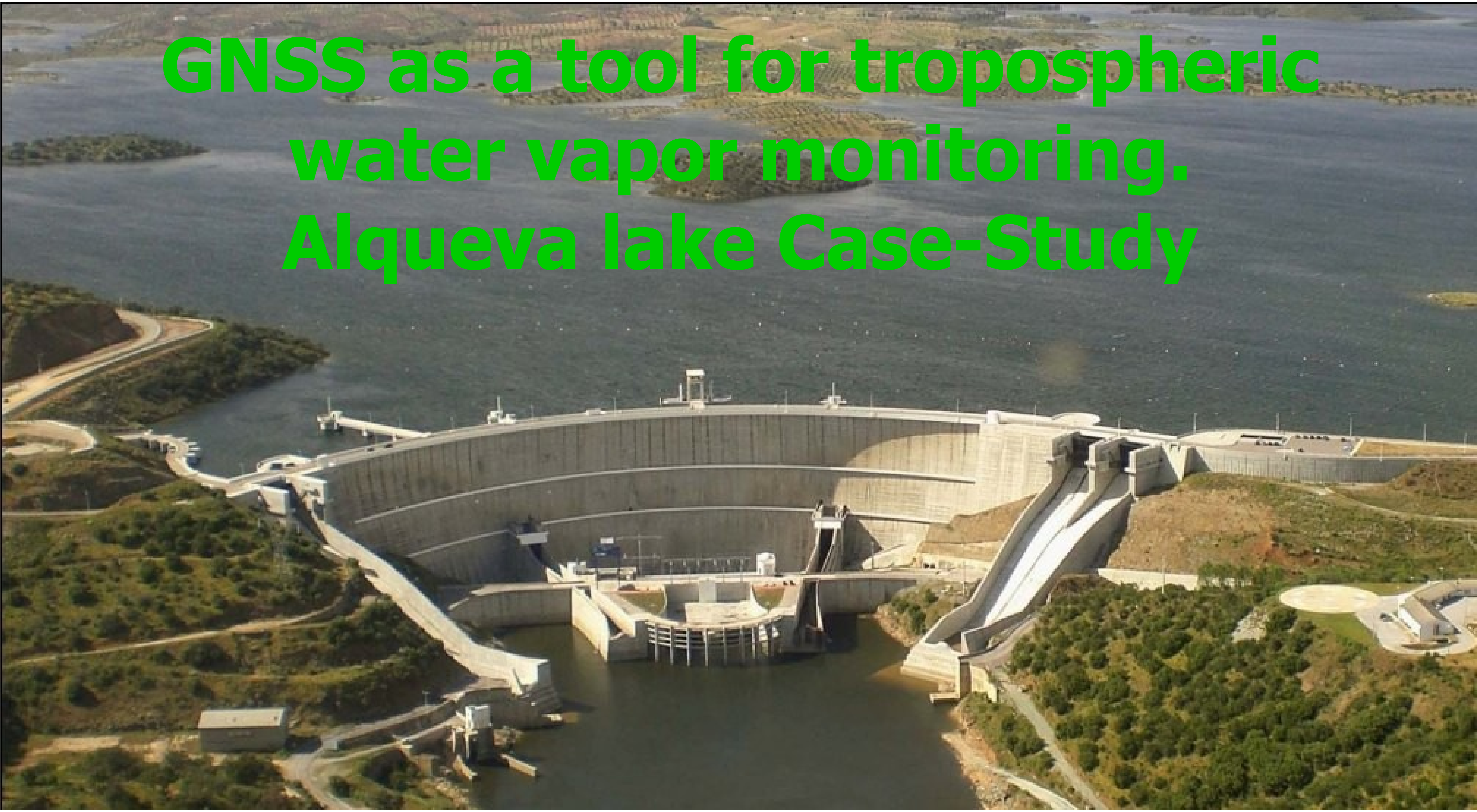

André Sá [1,2], Rui M.S. Fernandes[1,3], Fábio Bento[1], João Apolinário [1], Machiel Bos[1]
[1] SEGAL (UBI/IDL), Portugal; [2]UDI/ IPG ; [3]DEOS, TUDelft, The Netherlands

Outline

- Motivation
- Theoretical Introduction
  - GNSS, Atmosphere and Water Vapor
  - Signal Propagation in the Atmosphere, direct problem
  - Inverse Problem
  - GNSS Tomography
- ALEX 2014
- SWART Software
- Outlook and Summary

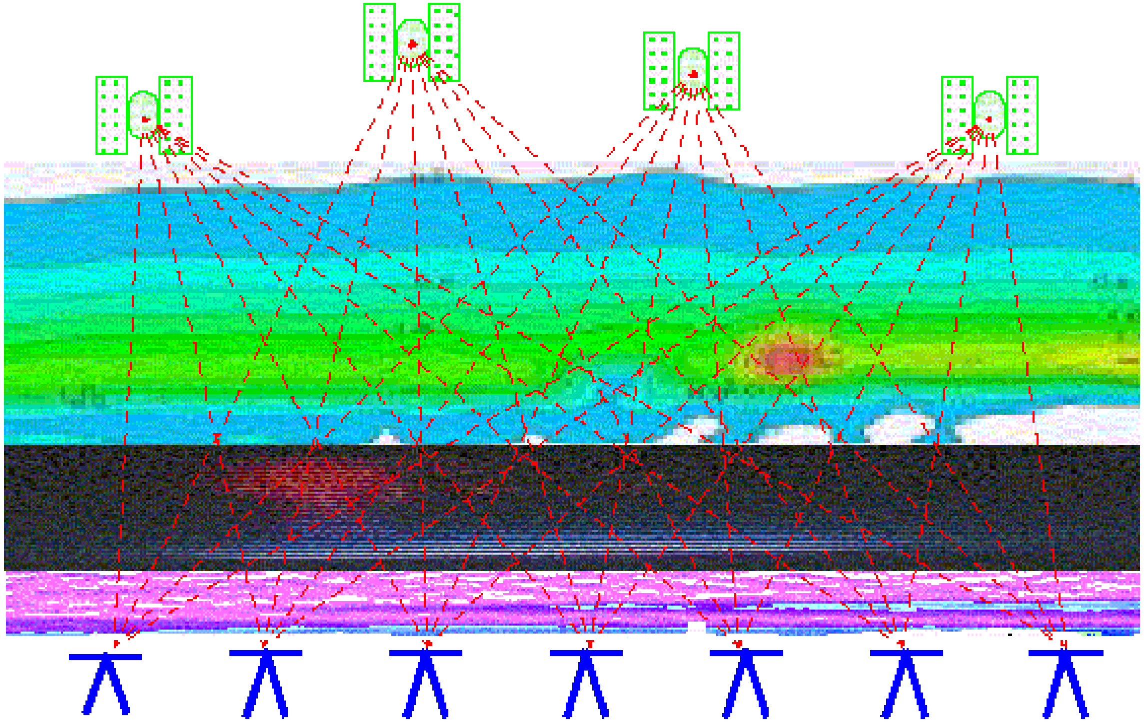

Motivation

Water vapor plays a crucial role in many atmospheric processes and is the most variable of the major constituents of the atmosphere. It has been proved the capabilities of GNSS technology to sense atmospheric water vapor. Major studies are strongly motivated by extreme weather events. What about other atmospheric patterns?

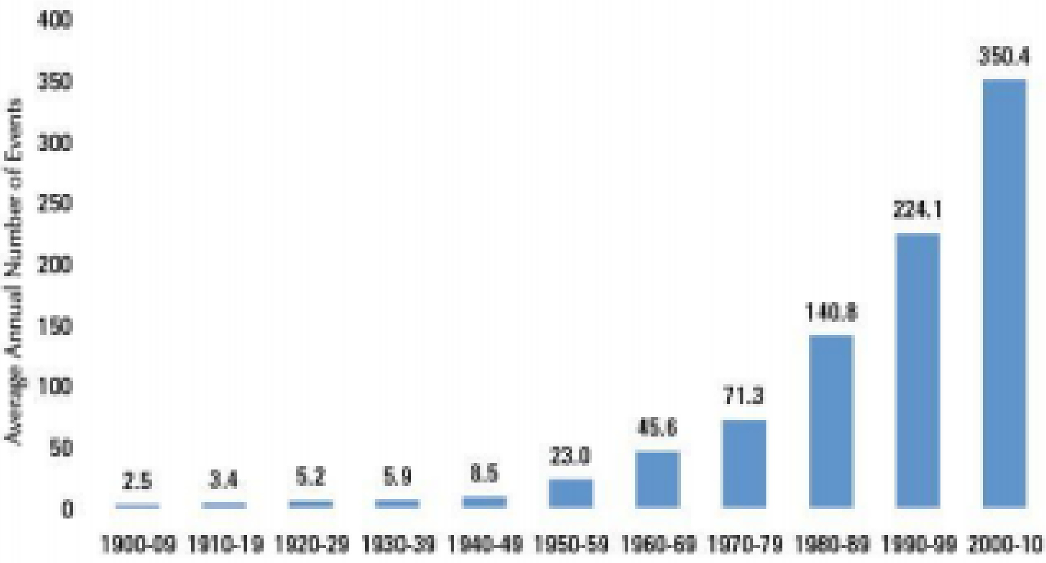

Figure 1: Average Number of Extreme Weather Events per Year by Decade, 1900–2010

Note: For the last period, 2000–2010, the annual number of events is based on an 11-year average. Statistics from the last "decade"—2000–2010—and the data for 2010 and perhaps even 2009 must necessarily be considered preliminary at this writing (March 2011).
Source: EM-DAT (2011).

Motivation

It is a system that works under all weather conditions, continuous unattended operation, good time resolution and an ever increasing number of stations.

- Soon more than 100 satellites in the sky

Motivation

- Identification of strong points and gaps in the tomography processing;
- Validate inversion techniques;
- Provide solid information on the accuracy of tomographic processing;
- Identify the potential use of tomography models;

↓

- Evaluate how to establish GNSS tomography as a standard sounding technique in Portugal;
- Contribute to COST Action ES1206 – Advanced Global Navigation Satellite Systems tropospheric products for monitoring severe weather events and climate (GNSS4SWEC).

Theoretical Introduction

- Receiver identifies each GPS satellite signal
- Position of GPS satellites known through broadcast ephemeris
- Travel time of signal between each satellite and receiver.

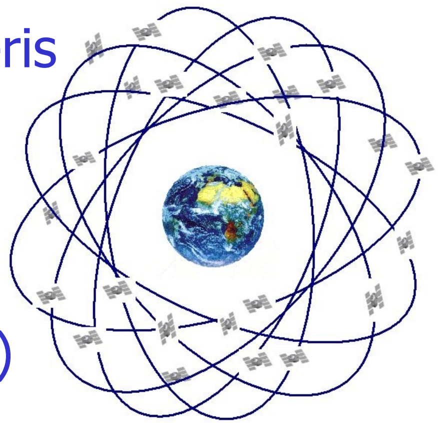

GNSS error sources

Satellite
- Orbit
- Clock
- Instrumental delays

Signal path
- Ionosphere
- Troposphere
- Multipath

Receiver
- Noise (code or phase)
- Instrumental delays

Antenna
- Phase center
- Elevation/azimuth
- Spoofing/interference
- Tides and loading
- Phase wind-up

Theoretical Introduction

Total Delay = Ionospheric Delay + Tropospheric Delay

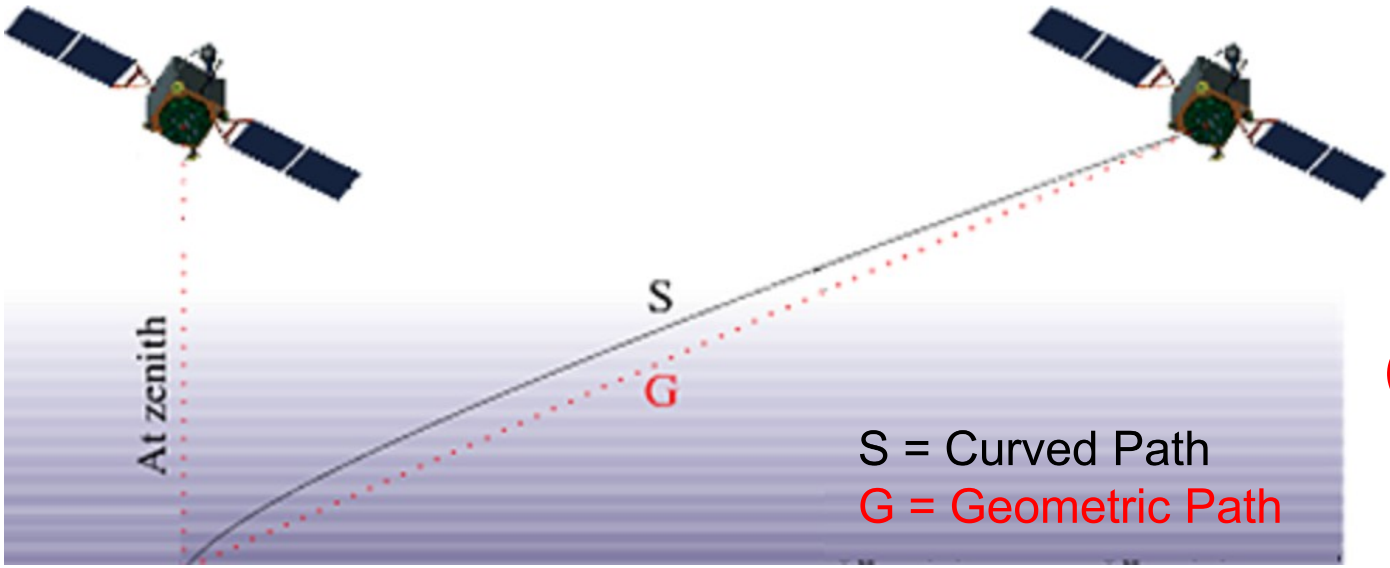

Noise (geodesy)

↓

Signal (meteorology)

Theoretical Introduction

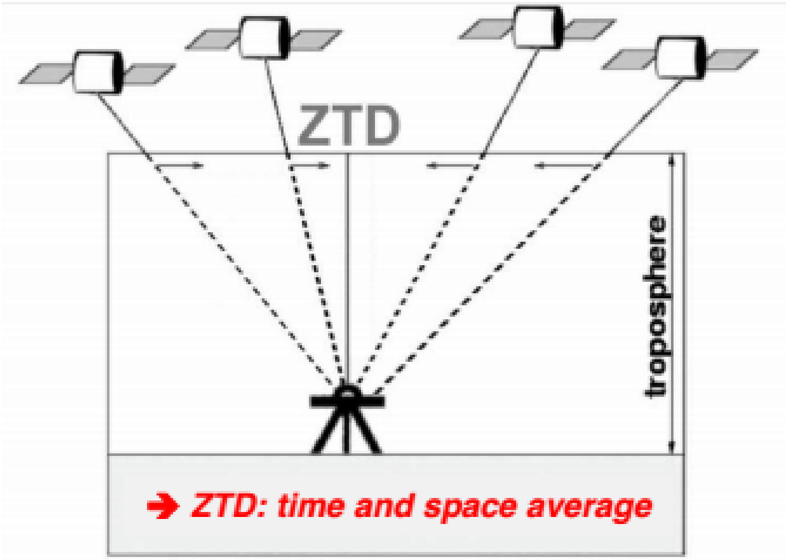

ZTD = ZHD + ZWD

« hydrostatic » délay — induced by all the neutral atmosphere

« wet » délay — specificity of the water vapour

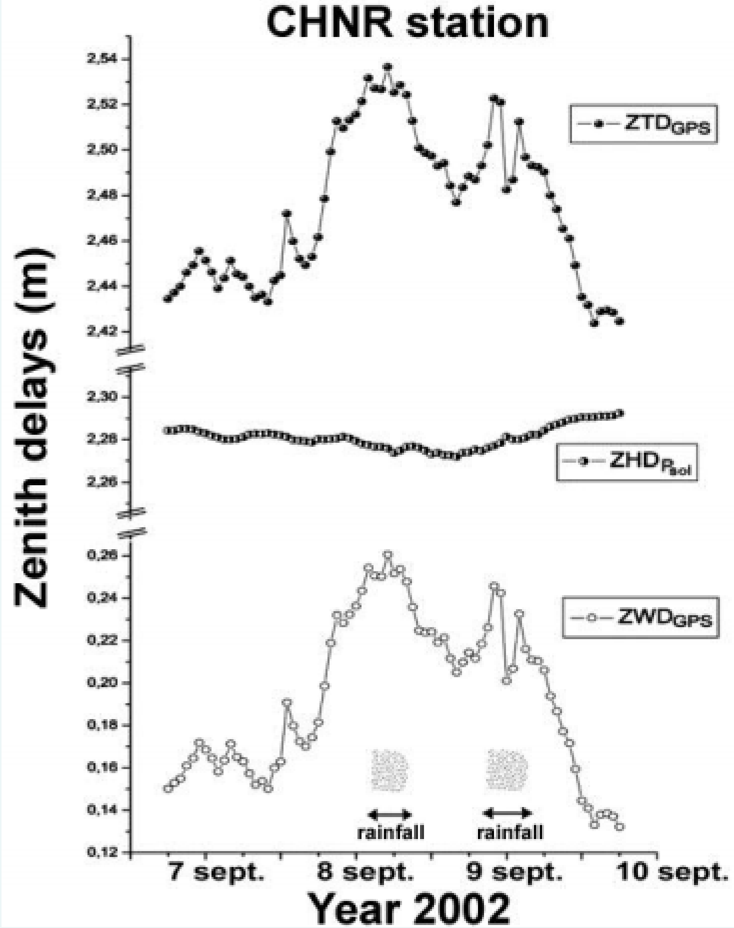

Theoretical Introduction

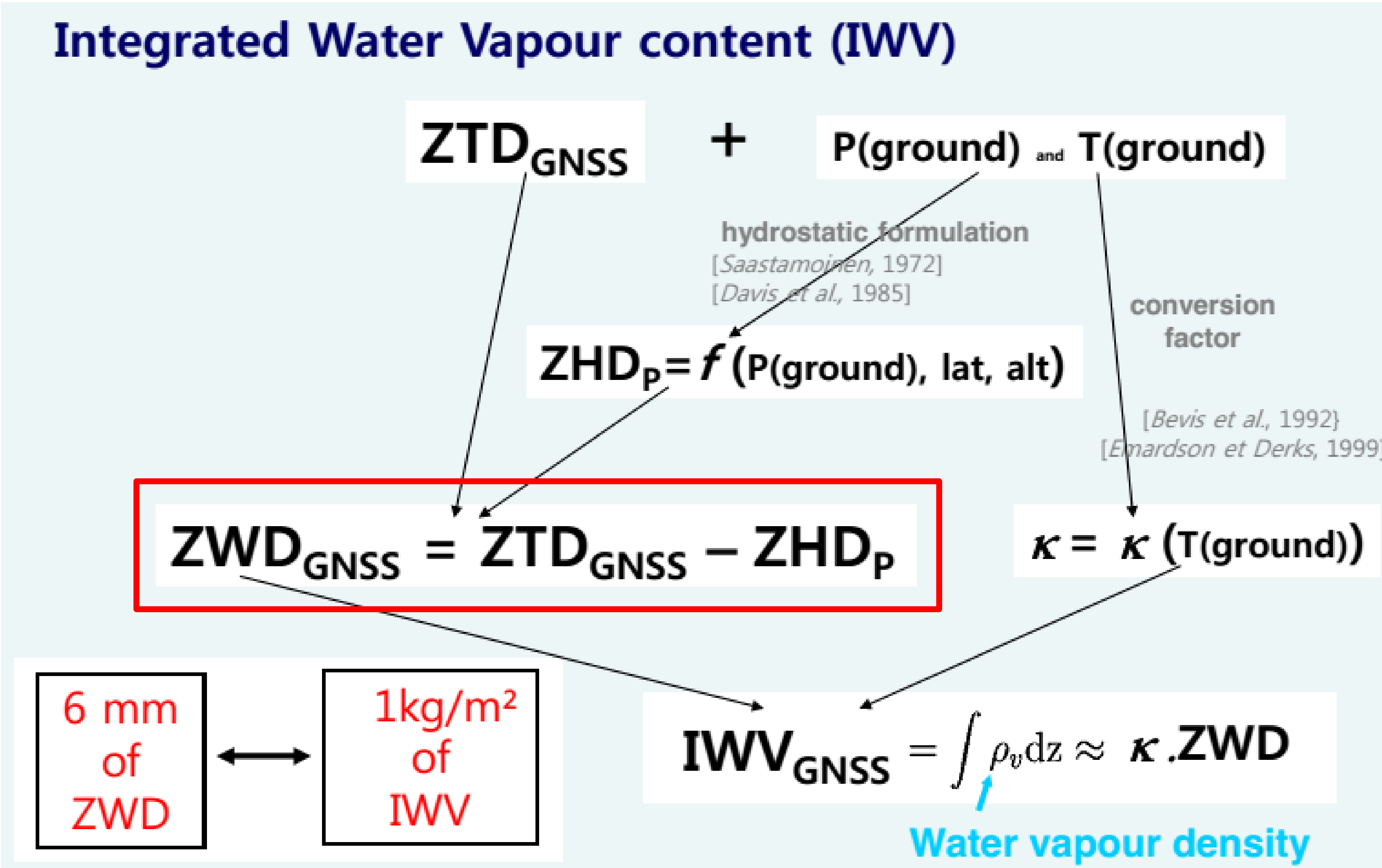

Theoretical Introduction

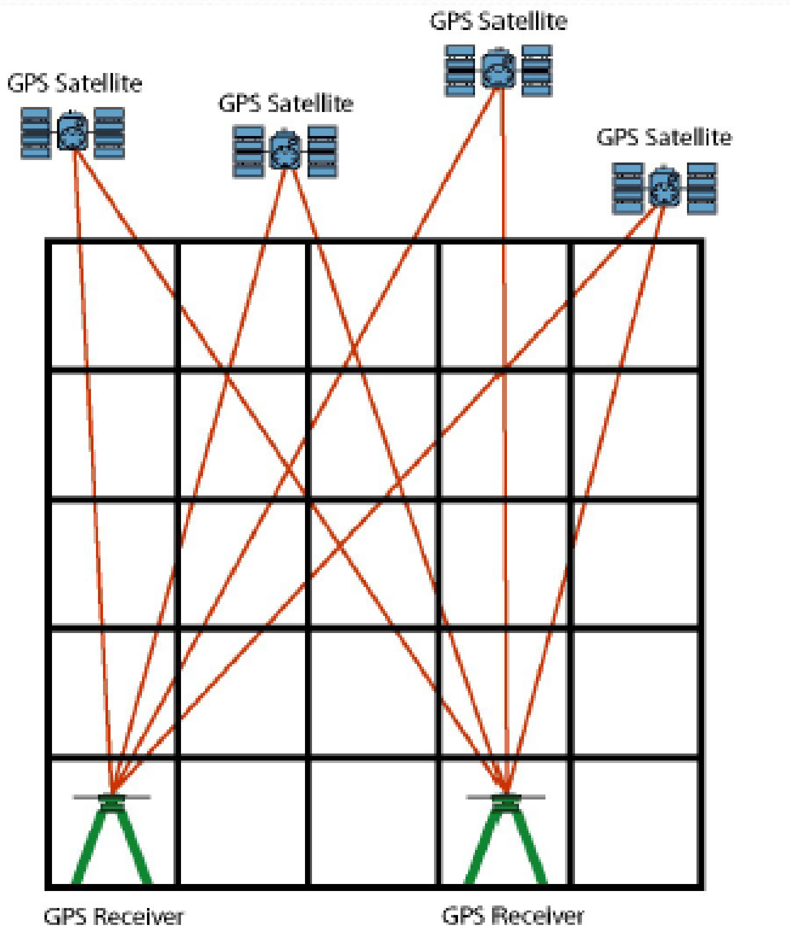

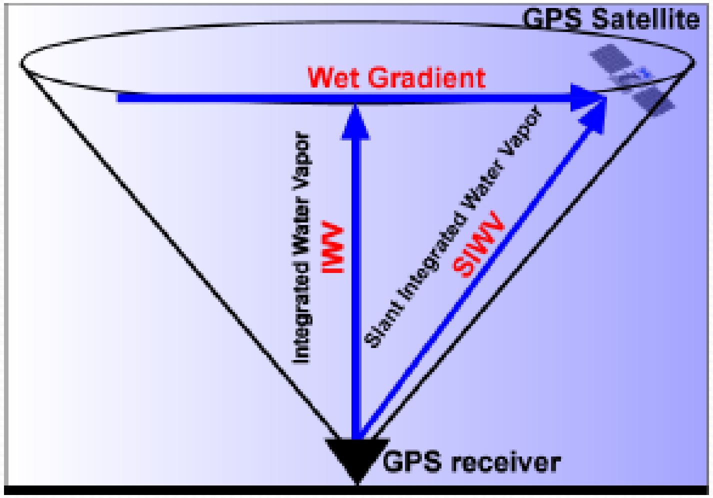

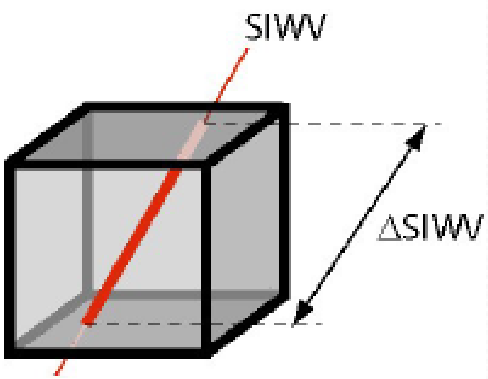

VOXEL

Theoretical Introduction

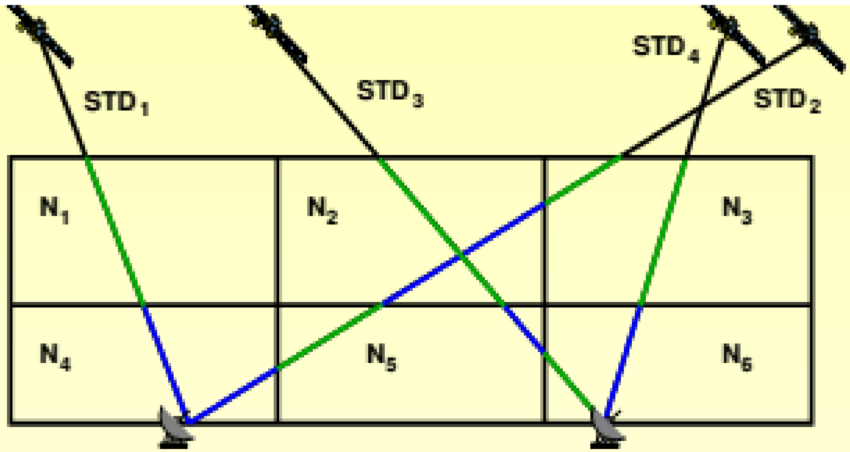

$$
\begin{aligned}
l_{11}N_1 + 0\cdot N_2 + 0\cdot N_3 + l_{14}N_4 + 0\cdot N_5 + 0\cdot N_6 &= STD_1\\
0\cdot N_1 + l_{22}N_2 + l_{23}N_3 + l_{24}N_4 + l_{25}N_5 + 0\cdot N_6 &= STD_2\\
0\cdot N_1 + l_{32}N_2 + 0\cdot N_3 + 0\cdot N_4 + l_{35}N_5 + l_{36}N_6 &= STD_3\\
0\cdot N_1 + 0\cdot N_2 + l_{43}N_3 + 0\cdot N_4 + 0\cdot N_5 + l_{46}N_6 &= STD_4
\end{aligned}
$$

$$
\begin{pmatrix}
l_{11} & 0 & 0 & l_{14} & 0 & 0\\
0 & l_{22} & l_{23} & l_{24} & l_{25} & 0\\
0 & l_{32} & 0 & 0 & l_{35} & l_{36}\\
0 & 0 & l_{33} & 0 & 0 & l_{46}
\end{pmatrix}
\cdot
\begin{pmatrix} N_1\\ N_2\\ N_3\\ N_4\\ N_5\\ N_6 \end{pmatrix}
=
\begin{pmatrix} STD_1\\ STD_2\\ STD_3\\ STD_4 \end{pmatrix}
$$

Theoretical Introduction

Standard techniques for solving linear inverse problems:

- Singular value decomposition
- Tikhonov-Regularization
- Conjugate gradient method
- Weighted least-squares solution
- Kalman-Filter
- Algebraic reconstruction techniques
- ...

ALEX 2014

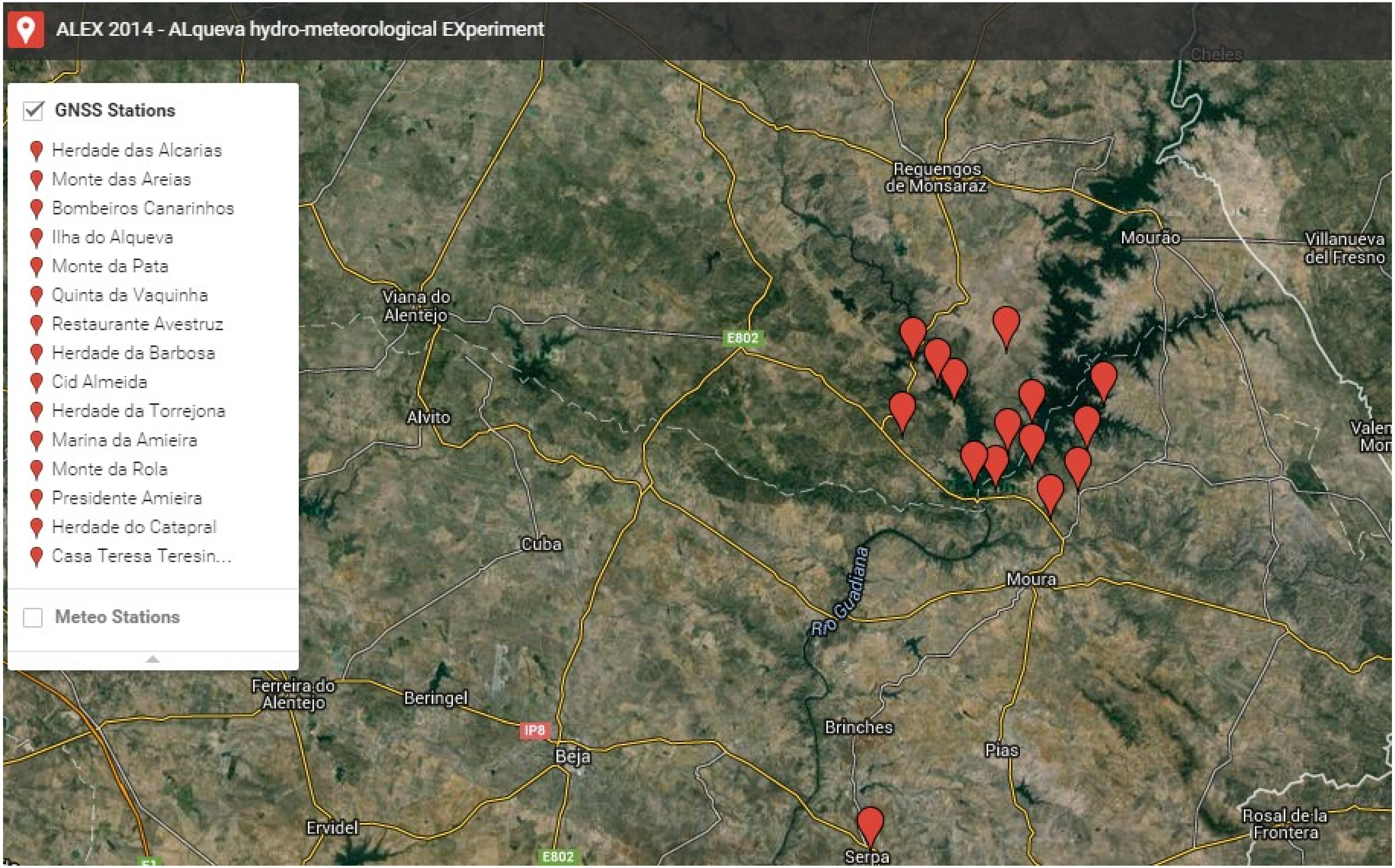

file:///C:/Users/Andre%20Sa/Desktop/Docs_A.Sa/Alqueva_GNSS_network.html

ALEX 2014 Results

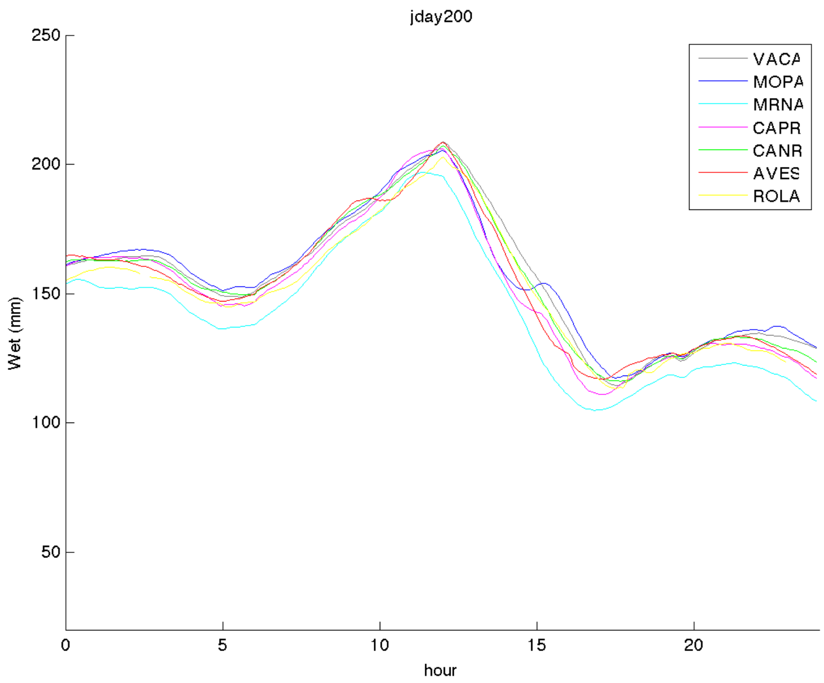

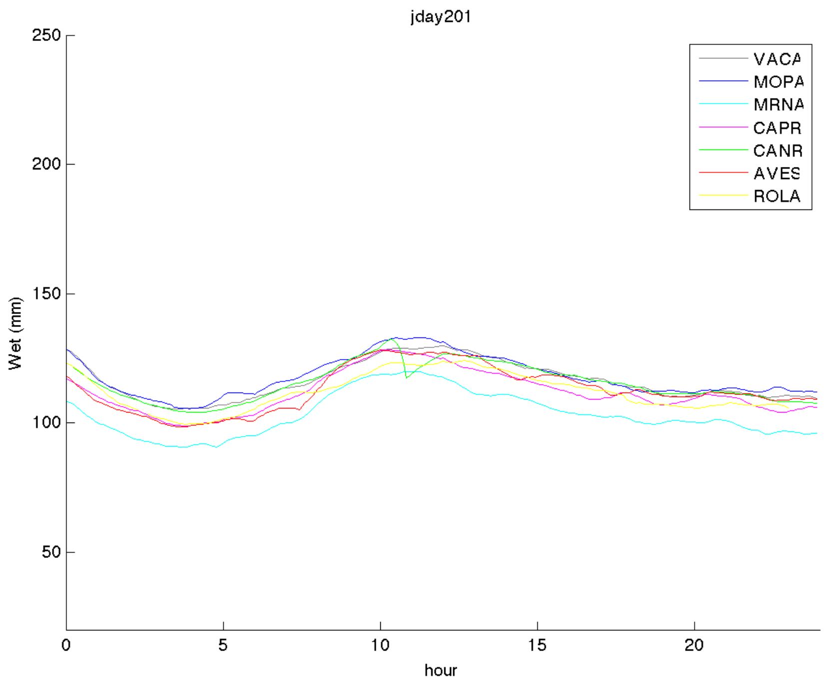

ALEX 2014 Results

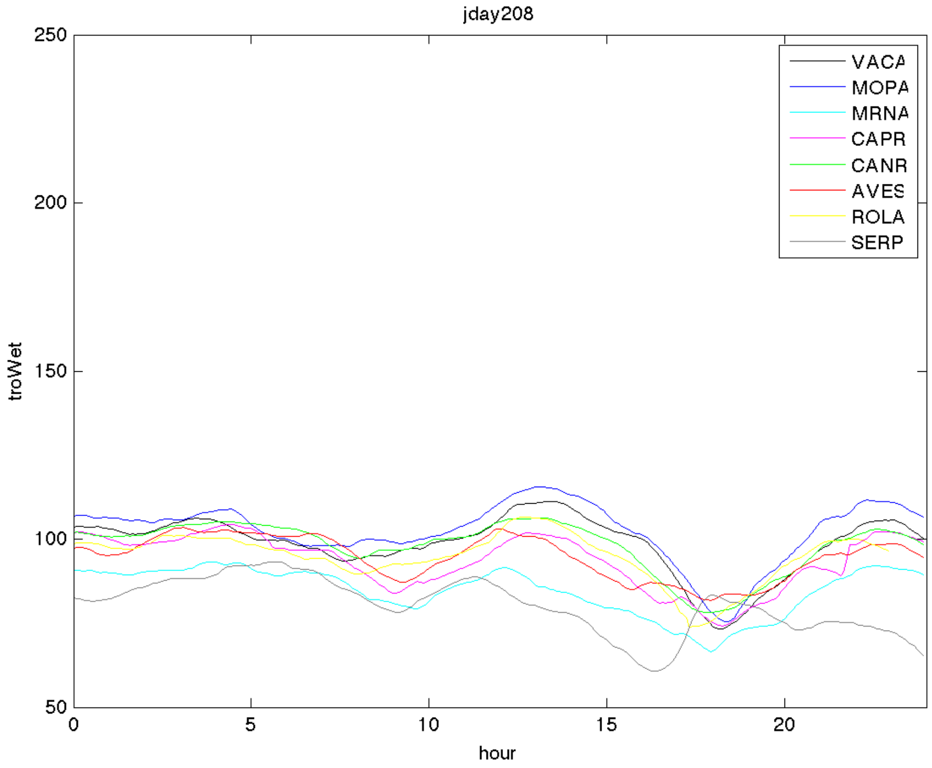

ALEX 2014 Results

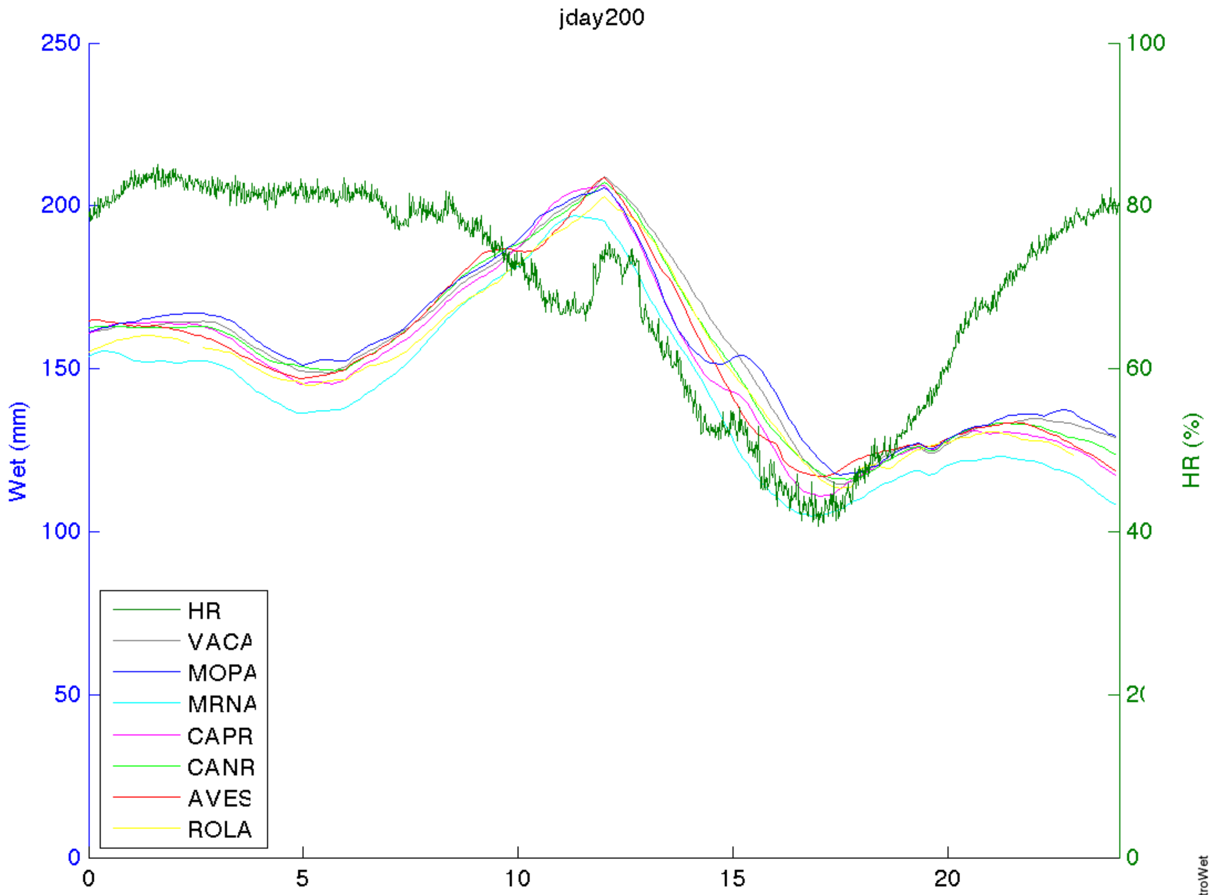

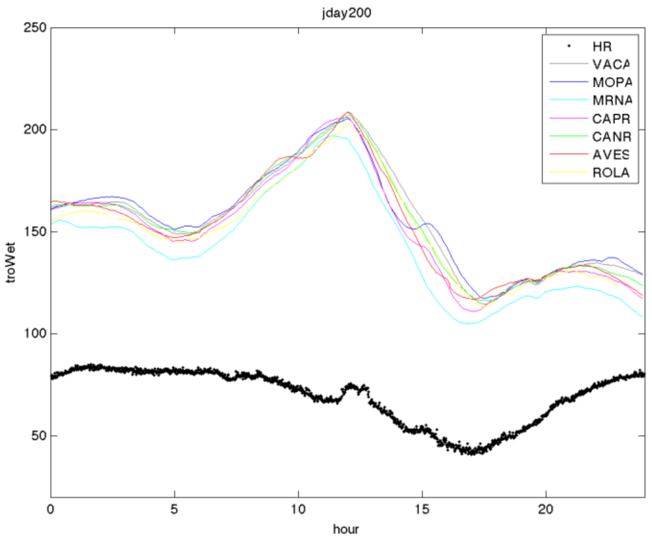

Rough correlation between humidity and GPS wet tropospheric delay

TOMOGRAPHY!

TOMOGRAPHY – SWART software

SWART – **S**EGAL GNSS **WA**ter Vapor **R**econs**T**ruction Image Software

- C++ software package
- For the inversion it uses Algebraic Reconstruction Techniques (ART)
- Diverse ART algorithms were implemented and parallelized on CPU and GPU

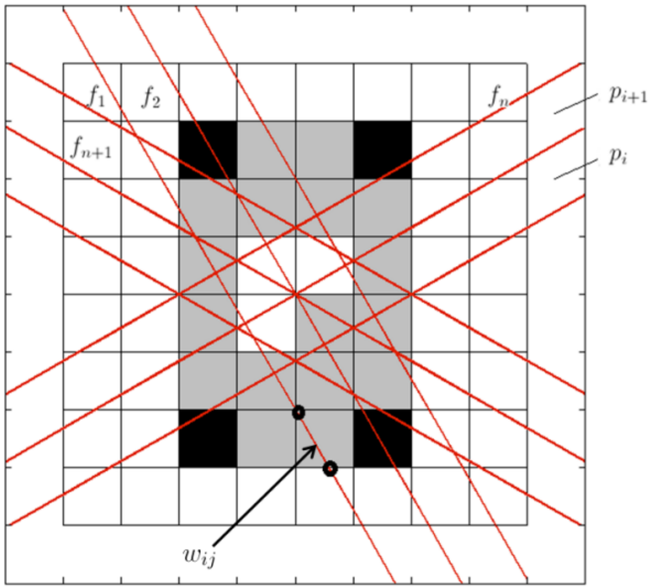

Shepp-Logan Phantom

Original Image

Kaczmarz CPU reconstruction

SART CPU reconstruction

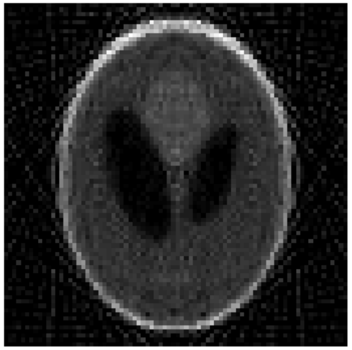

Landweber CPU reconstruction

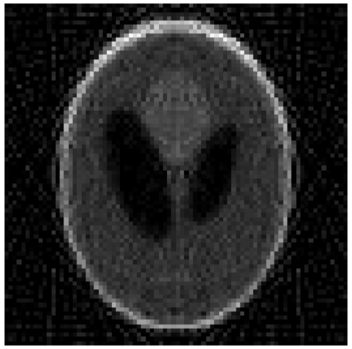

TOMOGRAPHY – SWART software

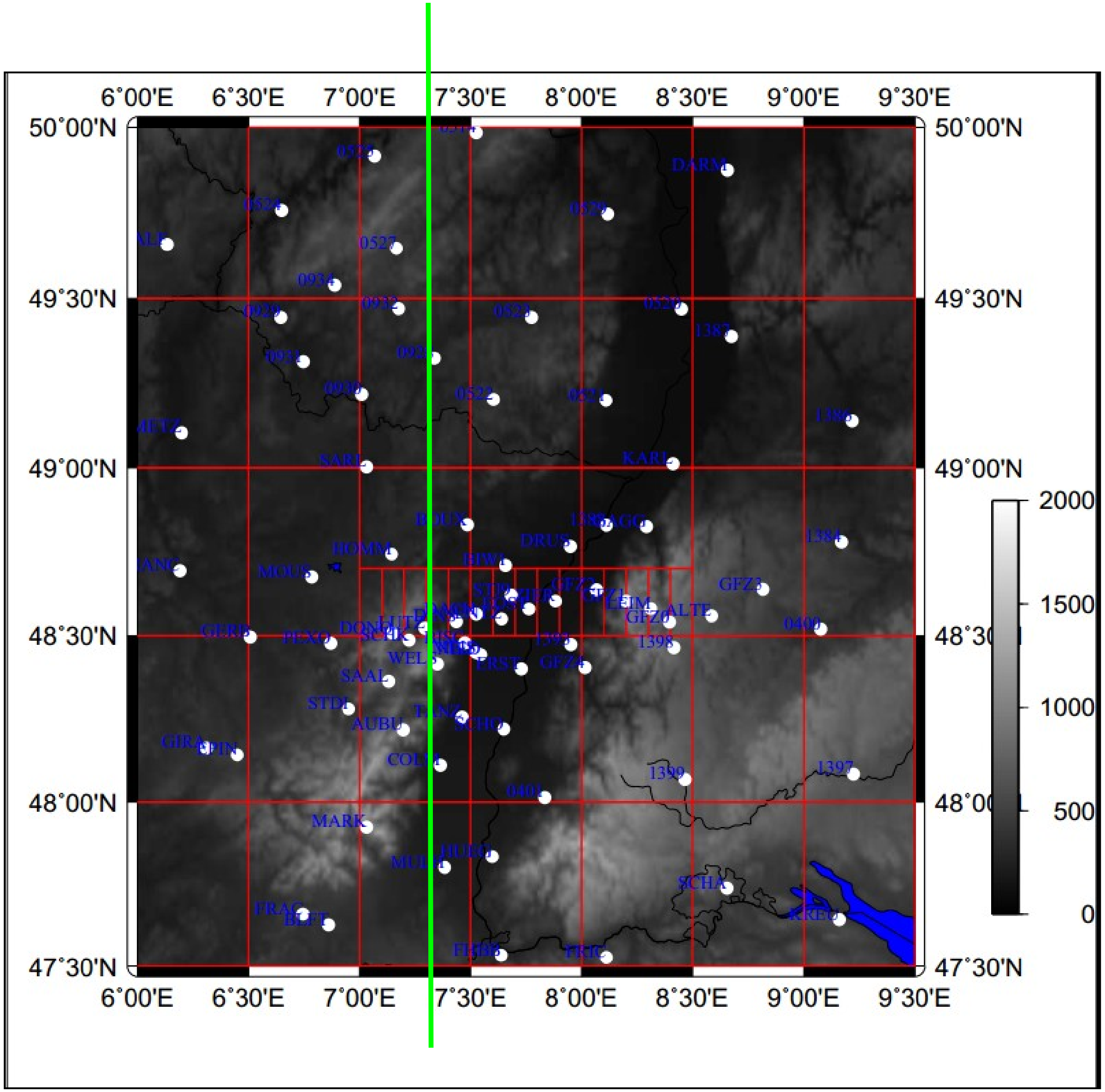

COPS France

Synthetic Data
85 stations

TOMOGRAPHY – SWART software

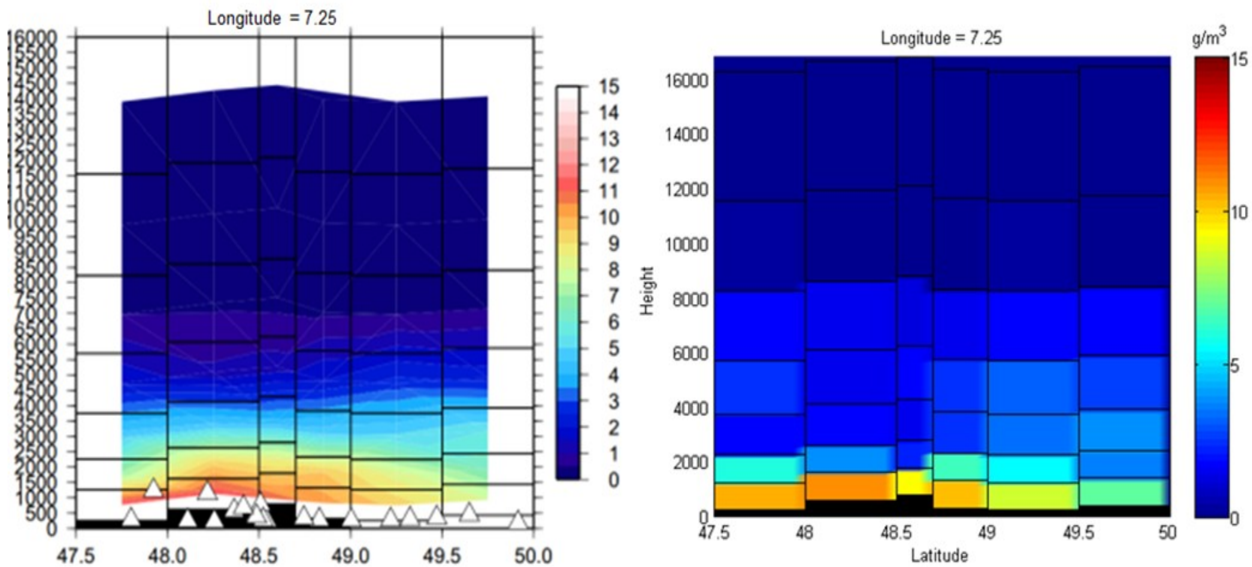

LOFTT_K and SWART results crossection showing the IWV content

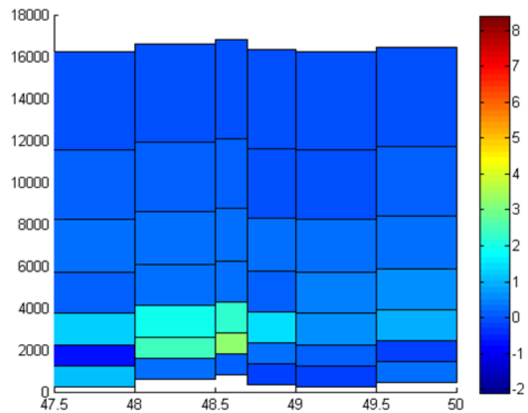

Differences between LOFFT_K and SWART in IWV values

TOMOGRAPHY – SWART software

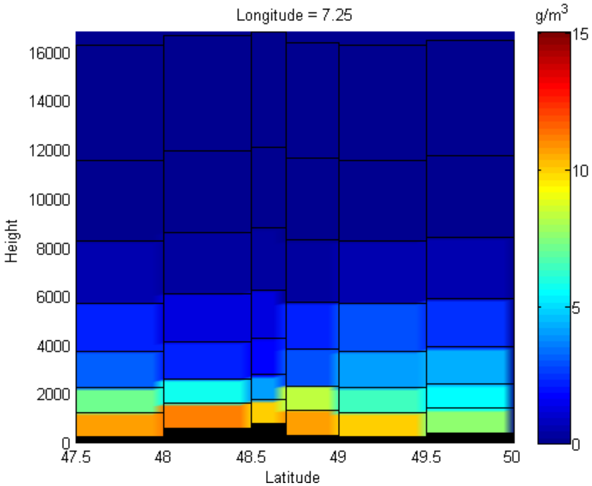

COPS 85 stations

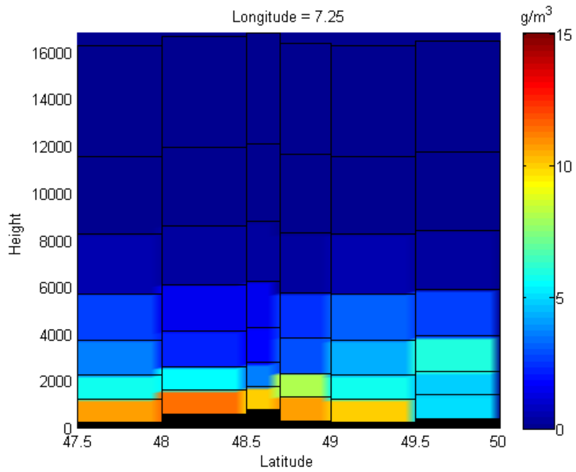

COPS 70 stations

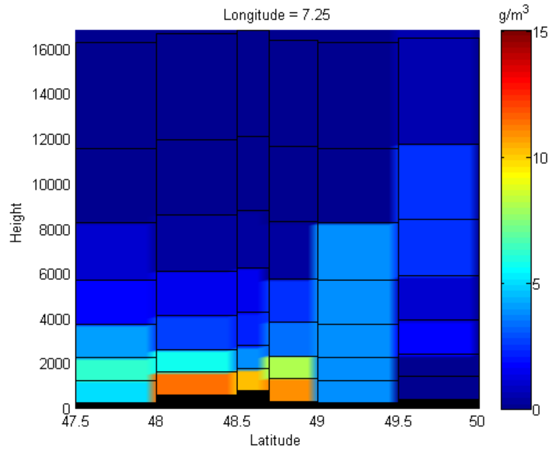

COPS 45 stations

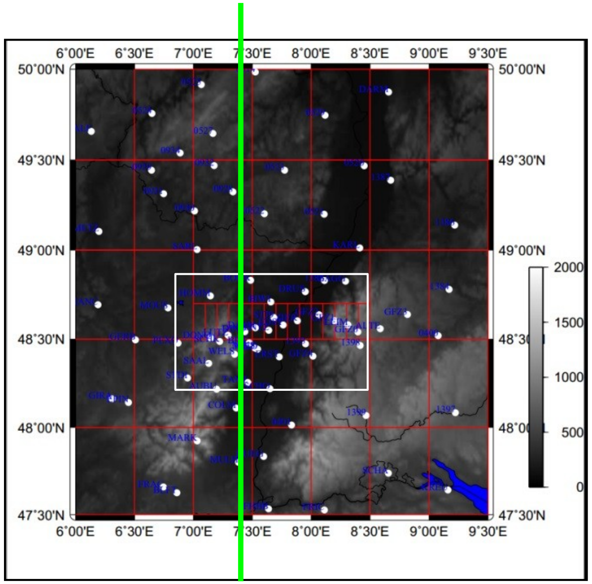

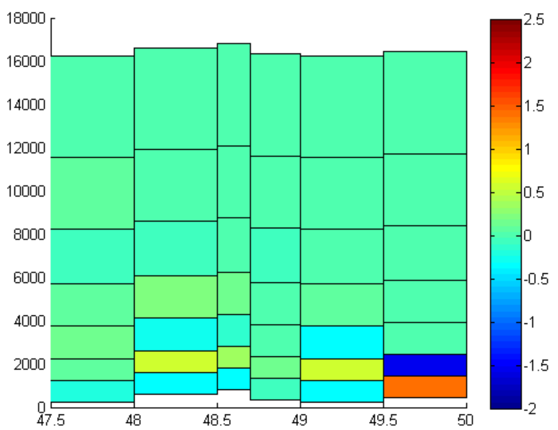
Swart diff 85-70 stations

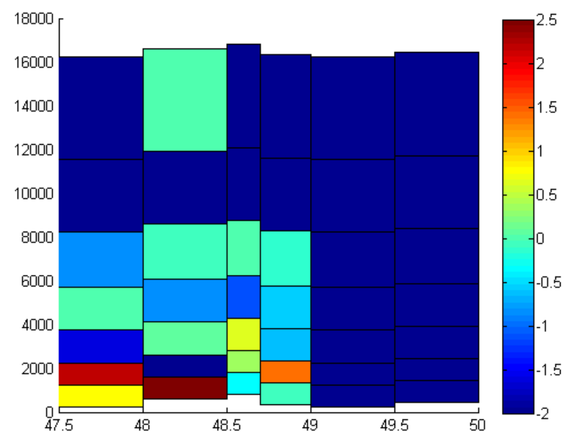
Swart diff 85-45 stations

TOMOGRAPHY – SWART software

Voxel Resolution

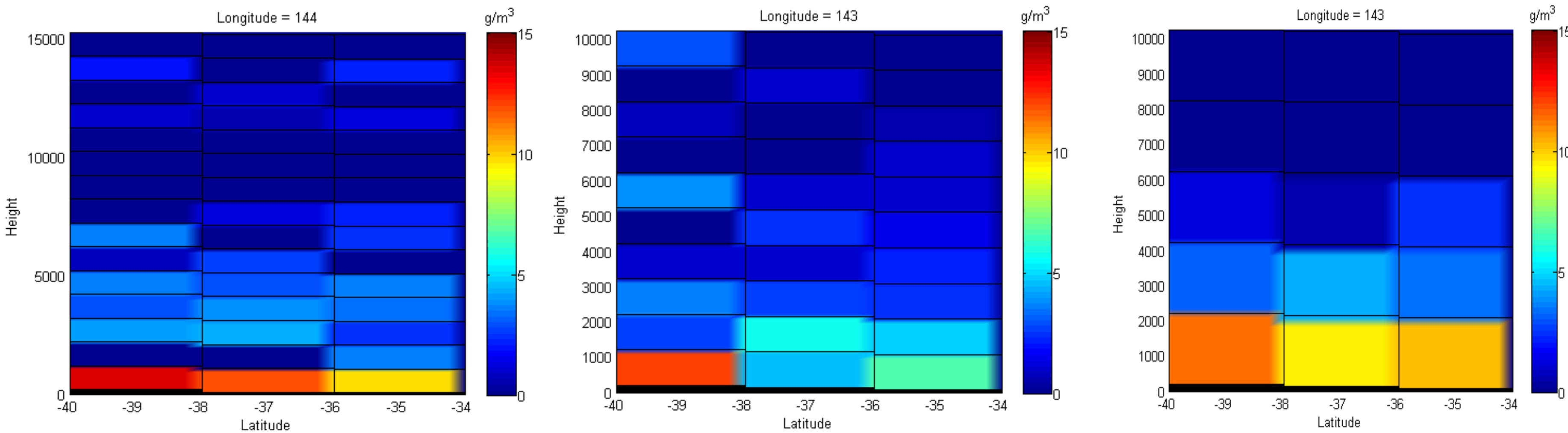

Integrated Water Vapor Characterization for different voxels resolutions

The results improve if we increase the size of the voxels (i.e., the number of voxels and unknowns decrease). Eventually, a stable and valid solution is reached but the main goal of the tomography is lost (Water Vapor vertical characterization/distribution).

TOMOGRAPHY – SWART software

Noise Test:

To check the influence in tomography of the noise in the observations, a basic test was performed: random noise was added to the slants wet delays.

Slant wet delays = Slant wet delays + (Noise/elAngle)
Noise = (random between -3% to 3%)*Slant wet delays

Random noise calculated in the loop, between -3% and 3% of each slant delay (slant wet delay * random function), divided by elevation angle to keep some proportion, since it's known that slants with low elevation angles present more delay and bending effect.

TOMOGRAPHY – SWART software

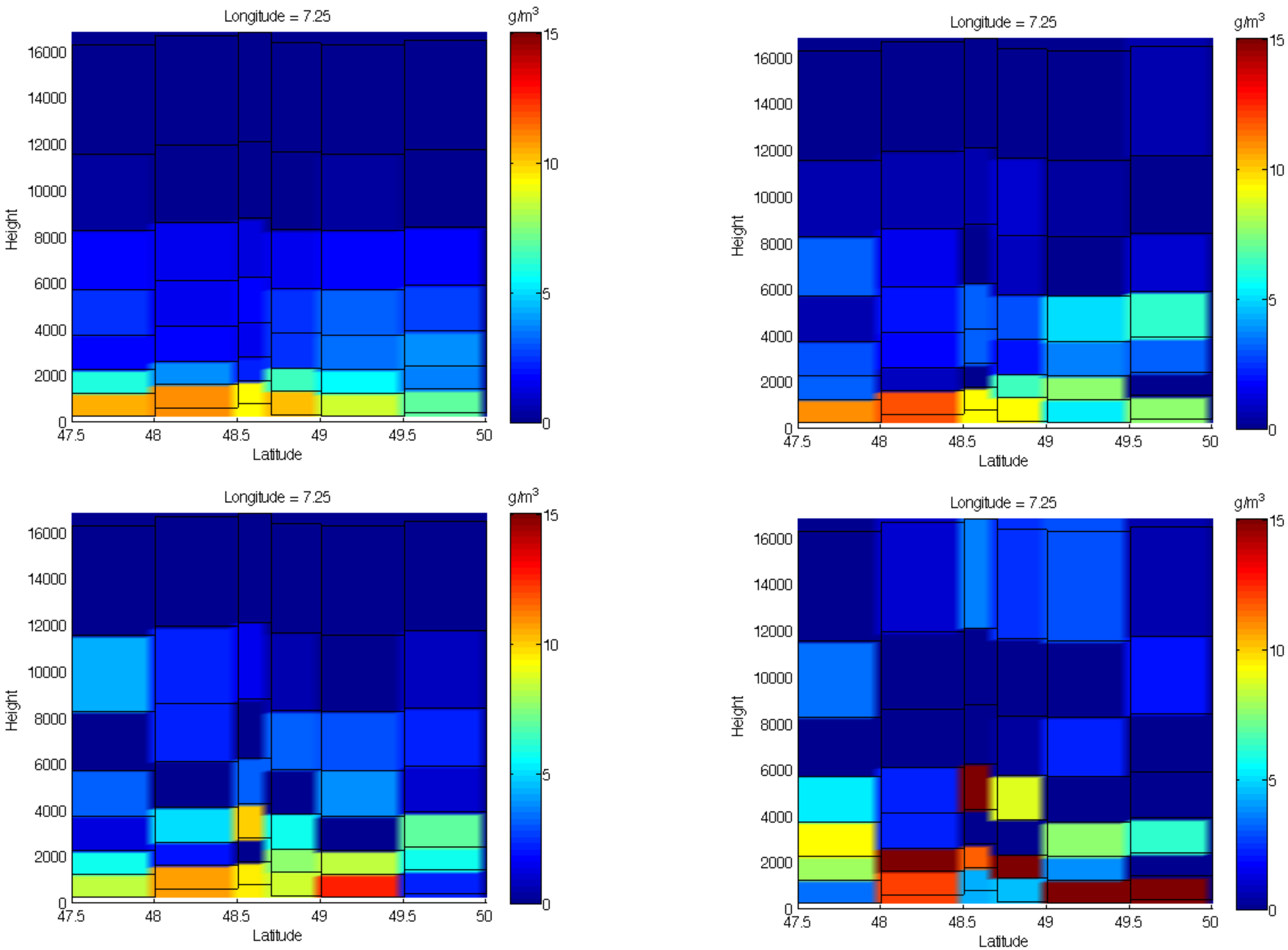

Integrated Water Vapor Characterization: top left) without noise; top right) 3% of random noise; bottom left) 5% of random noise; bottom right) 10% of random noise.

TOMOGRAPHY – SWART software

Back projection

To verify the state of **x** between the synthetic and real data the back projection technique was applied.

$$\mathbf{Ax = m}$$

m in equation represents the observations (slants path delays). If we use the computed **x** to retrieve **m** (**mSWART**):

$$\textbf{residuals} = \mathbf{m} - \textbf{mSWART}$$

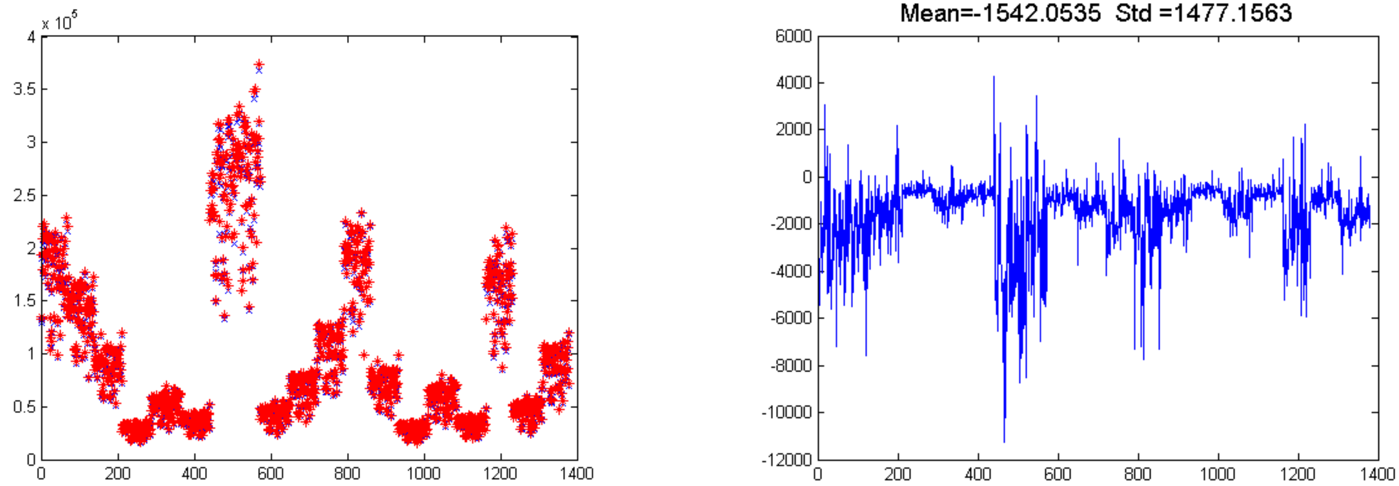

Back projection with synthetic data, slants (left) and residuals (right), the red dots show the back projection while blue dots the original slant data

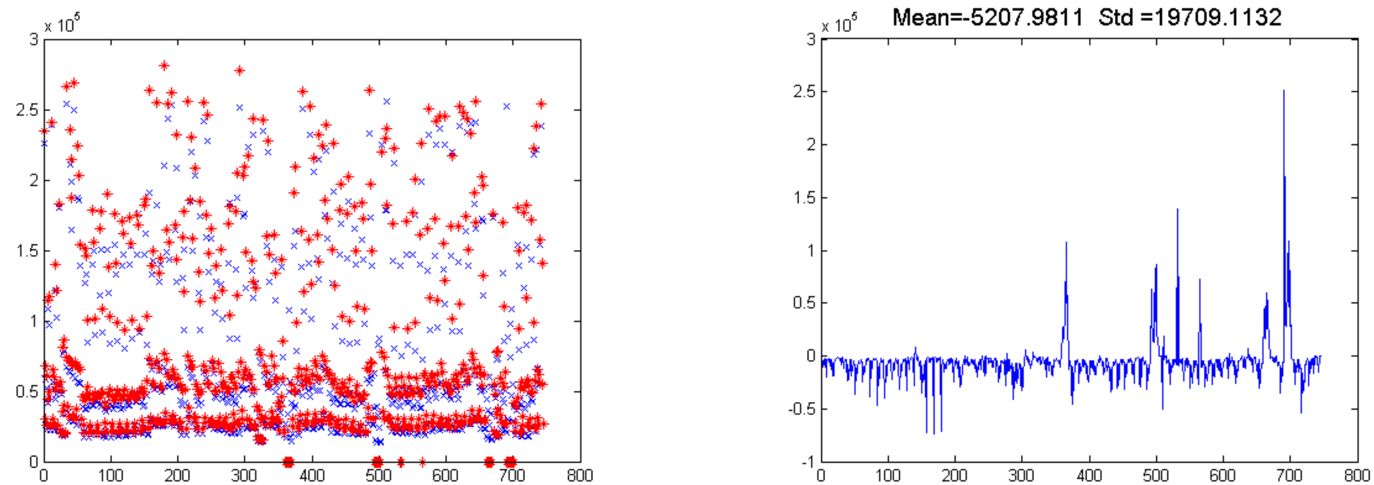

Back projection with real data (Australia network), slants (left) and residuals (right), the red dots show the back projection while blue dots the original slant data.

Tomography Results!

Belem network

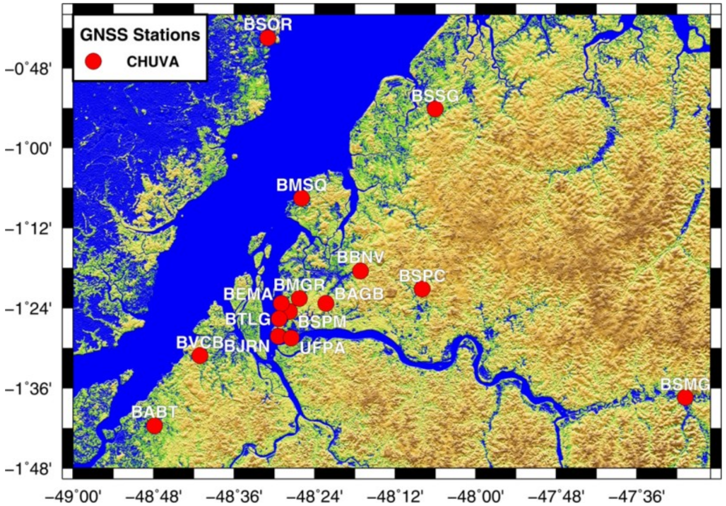

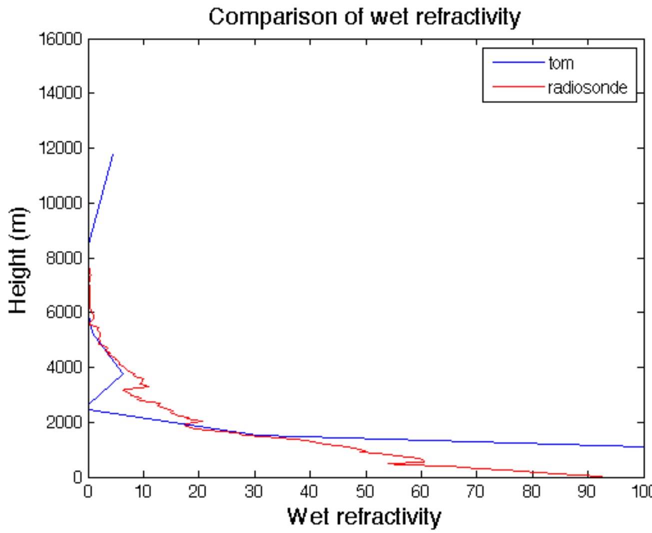

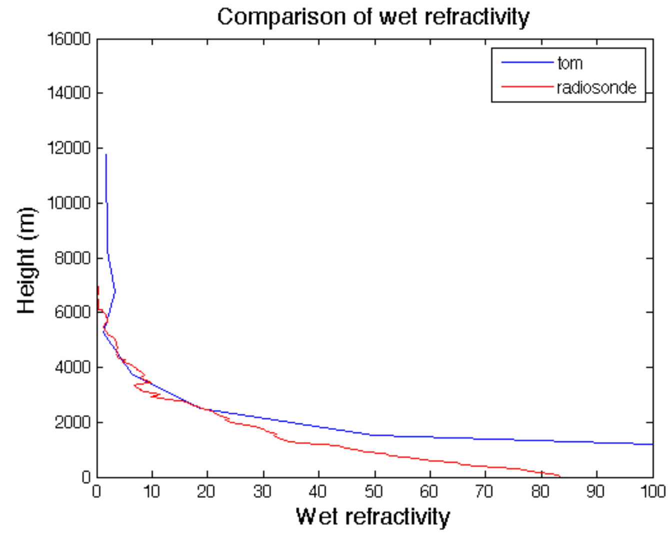

Due to configuration network and no altimetry difference between the stations (43 m maximum), the tomographic results present unrealistic values on the bottom layers. The bottom layer with low number of rays intersections and very limited angular variability of the rays due to rather flat terrain in the study region tend to accumulate the total water vapor from the whole model.

Outlook

- GNSS can be a meteorological sensor.
- Quality of the GNSS tomography is affected by a number of factors such as spatial-temporal distribution of the observations, grid resolution, the reconstruction method, the initial field, terrain morphology.
- Independent observations can help to constrain the apriori GNSS tomographic field.
- Some constraints needs to be considered: Initial field, relaxation parameter λ used to weight the result of the reconstruction against the initial value; At the upper level of the grid the humidity can be assumed to be near zero at least if the tomography reaches the tropopause (>10km) and inter-voxels constraint limiting the difference between neighboured voxels.

Questions!

the end…

SWART-Number of iterations

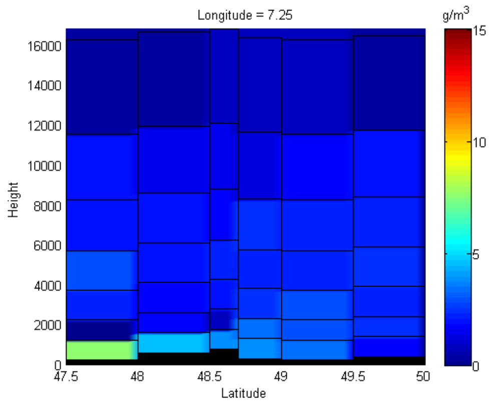

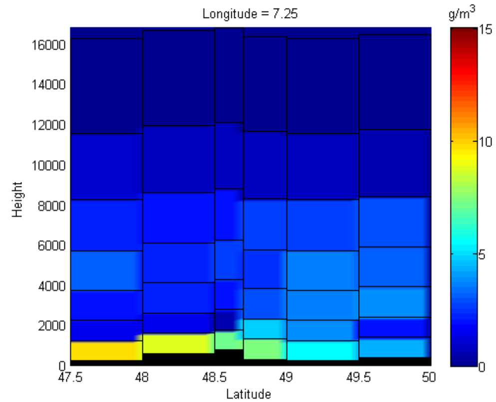

SWART results using synthetic data for 100 (left) and 1000 (right) iterations

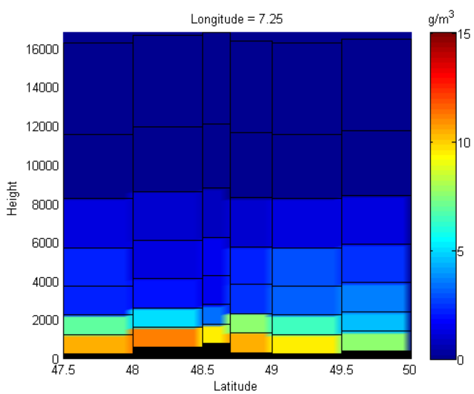

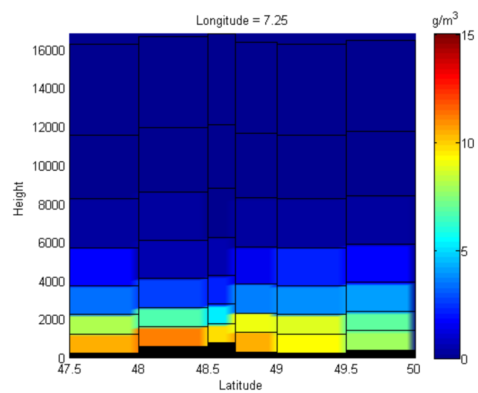

SWARTS results for 10000 (left) and 100000 (right) iterations

SWART-Number of iterations

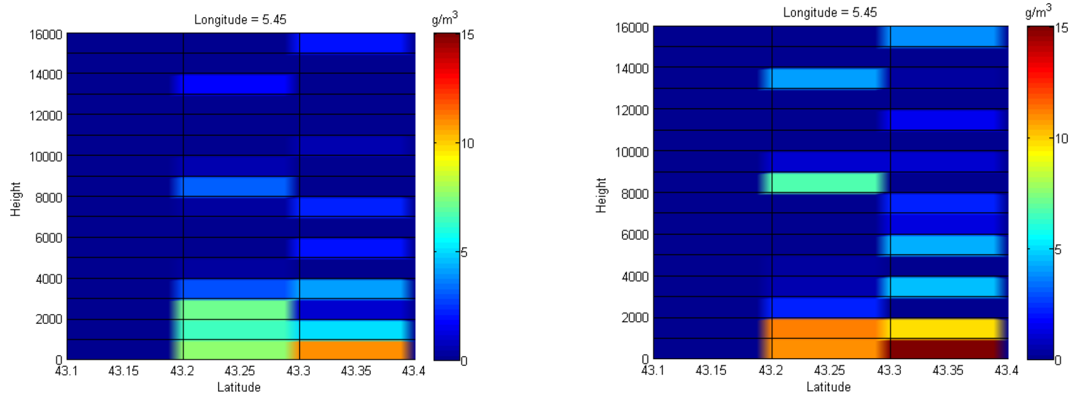

SWART results using real data for 1.000 (left) and 10.000 (right) iterations

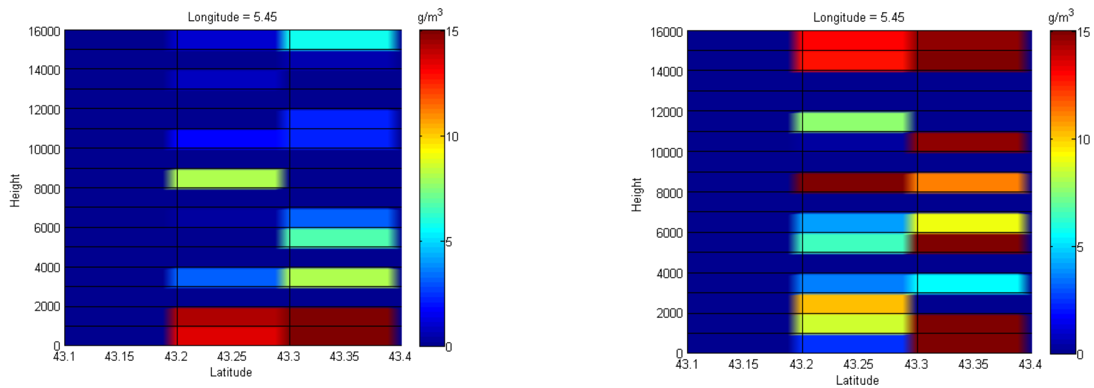

SWART results using real data for 100.000 (left) and 1.000.000 (right) iterations

Therefore, criteria have to be defined in order to describe the convergence behavior and to be used to stop the iteration in an optimal way. Based on the back projection $A * x^k = m^k$ is close to the experimental data $m = m^0$, i.e., $|m_0 - Ax^k| = min.$

In general, a solution $\mathbf{x}$ with $\mathbf{A}\mathbf{x} = \mathbf{m}$ does not exist, therefore find $\tilde{\mathbf{x}}$ which minimizes the norm

$$\min \{ \, ||\mathbf{A}\mathbf{x} - \mathbf{m}|| \, \} \quad \text{subject to} \quad ||\mathbf{x}|| \leq \alpha$$

Standard techniques for solving linear inverse problems:

- Singular value decomposition
- Tikhonov-Regularization
- Conjugate gradient method
- Weighted least-squares solution
- Kalman-Filter
- Algebraic reconstruction techniques
- ...

SWART- Initialization Values

No initialization values and 50000 iteractions

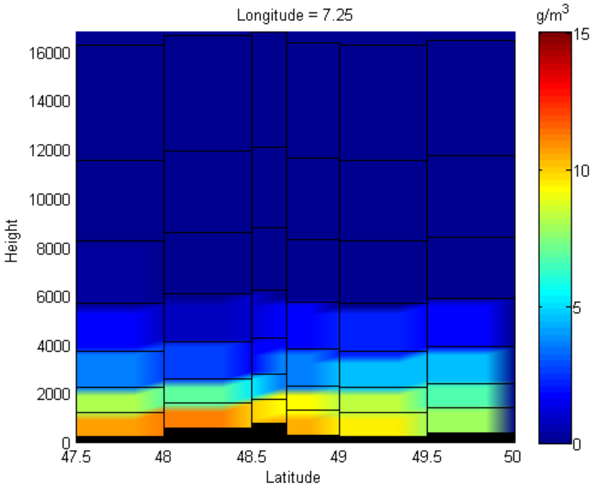

Kaczmarz

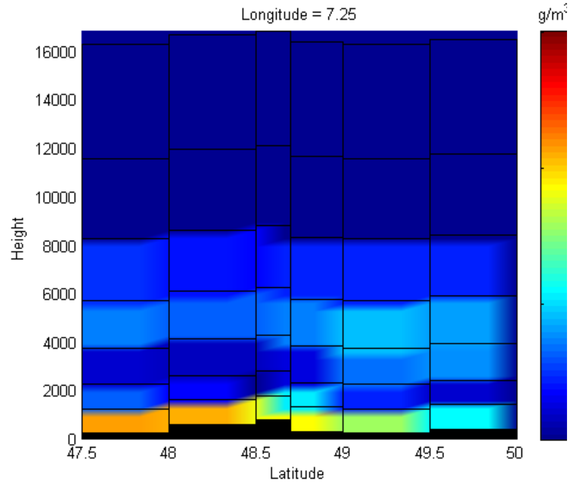

Landweber

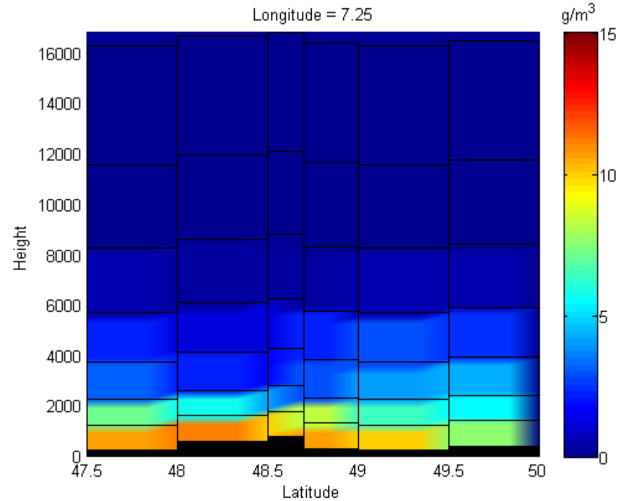

SART

Initialization values 15 under 2500 m and 50000 iteractions